Progress In Electromagnetics Research C, Vol. 16, 25–35, 2010

PYTHAGORAS TREE: A FRACTAL PATCH ANTENNA FOR MULTI-FREQUENCY AND ULTRA-WIDE BANDWIDTH OPERATIONS

A. Aggarwal and M. V. Kartikeyan

Department of Electronics and Computer Engineering
Indian Institute of Technology
Roorkee 247667, India

Abstract—This paper shows the design of a fractal patch antenna, which uses a unique fractal geometry known as Pythagoras tree with co-planer waveguide (CPW) feeding. The antenna has been designed for dual band operation at the WLAN/WiMAX (2.4 GHz) and WiMAX (3.5 GHz) for ultra-wide bandwidth applications. The antenna was simulated using CST Microwave Studio. The fabricated antenna's measurement results were found to be in good agreement with the simulated ones.

1. INTRODUCTION

Antennas have been studied for about a hundred years and in use for as long. Fractal shaped antennas are used today for multi-frequency purposes which was not possible for traditional antennas. As microstrip patch antennas are low profile, compact, low manufacturing cost and easy integration on MMIC, they are most favorable among all antenna designs.

Wireless applications at low frequencies are always a quite difficult task for engineers as the wavelength of the antenna is in direct proportion to its size. So, at low frequencies the antenna of smaller size is always a preference. The main aspect needed in today's communication is the multiband behavior of the device as antenna, etc. There are antennas which show dual band [1, 2] behavior by using techniques such as slots [3], arrays [4], etc. The recent work done is on the stacked patch antennas with U-slots and fractal defects [13] along with the full ψ-shaped and half ψ-shaped microstrip patch

Received 22 June 2010, Accepted 23 August 2010, Scheduled 9 September 2010
Corresponding author: M. V. Kartikeyan (kartik@ieee.org).

antennas [5], but having more than two or three frequency band operations is difficult by just using slots, so today a new technique is used for such applications, i.e., the use of fractal geometries [6] instead of normal rectangular or square patches. Today, fractal geometries due to their space filling properties are widely used in miniaturization along with other advantages as multiband operation, impedance matching [7, 8, 14].

In this paper, a fractal patch antenna using Pythagoras tree as the fractal geometry is presented for dual frequency ultra-wide bandwidth operation. The existence of infinite fractal geometries and their advantages opens the door to endless possibilities to accomplish the task at hand. The use of fractals provides us with a bigger set of parameters to control the antenna characteristics. The antenna designed works on 2.4 GHz and 3.5 GHz WiMAX band, which is a next generation internet access network [9, 10].

2. ANTENNA GEOMETRY AND CONFIGURATION

The antenna geometry, Pythagoras Tree, is a plane fractal constructed from squares. It is named after Pythagoras, because each triple of touching squares encloses a right triangle, in a configuration traditionally used to depict the Pythagorean Theorem. The same procedure is then applied recursively to the two smaller squares. Figure 1 below shows the first three iterations in the construction process. The dimension of the basic square is chosen from the rectangular patch antenna for the 2.4 GHz operating frequency.

Figure 2 shows the antenna configuration. The patch with 50 Ω CPW feeding as shown in Figure 2 is simulated. The antenna is fabricated on the Netlec NH9338 ($\varepsilon_r = 3.38$) substrate with substrate thickness $t = 1.524$ mm (60 mil) and loss tangent $\tan\delta = 0.0025$. Now, the angle between one bigger and one smaller consecutive patch is kept constant at 45°. So, the dimension of all the smaller patches

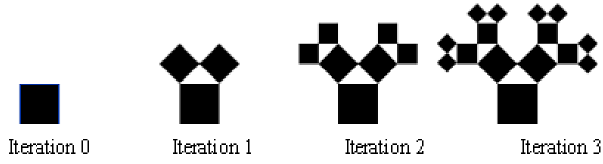

Figure 1. Pythagoras tree generation after first three iterations (dimensions in mm).

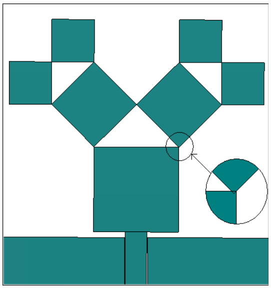

Figure 2. Simulated antenna design using CPW feeding.

depends on their immediate bigger neighbour patch. The size of the bigger patch ($2 * pl$) is 63.34 mm. The substrate dimension is $sd * w\_sd = 106.5\,\text{mm} * 100\,\text{mm}$. The width of the CPW feed is $wf = 8\,\text{mm}$. The gap between CPW feed and ground plane is $gps = 0.32\,\text{mm}$ while the gap between the ground plane and the patch is $gpd = 2.1\,\text{mm}$. The geometry shows multi-band and wide bandwidth behaviour compared with the existing square patch of same dimensions.

3. RETURN LOSS AND PARAMETRIC STUDY

The antenna is simulated and fabricated for the above configuration. The simulated and measured return losses are as shown in Figure 3 and Figure 4 respectively. The simulated antenna shows dual band operation for two different wireless applications. The antenna operates at 2.4 GHz WLAN/WiMAX and 3.5 GHz WiMAX. The bandwidth at 2.4 GHz is around 750 MHz, and at 3.5 GHz is around 1.342 GHz as shown in Figure 3.

Figure 4 shows the measured return losses of the printed antenna. The fabricated antenna results are found to be in good agreement with the simulated ones. The parameters "wf" and "gps" are calculated using CPW 50 Ω matching line formulas as stated in [11]. The values of "wf" and "gps" are 8 mm and 0.32 mm respectively. Now the parametric study of the rest of the antenna parameters is carried out, and the parameters which are affecting the antenna characteristics are patch length 2∗"pl", distance between ground and patch "gpd" and substrate dimension. The substrate dimension in this case is varied in all the four directions. The dimension varied in left and right is the same and represented as "w_sd" as it is along the width of the patch while the dimension containing the CPW feed is represented as "sdf", and the dimension opposite to CPW feed is represented as "sd". The parameter "pl" controls the antennas operating frequencies

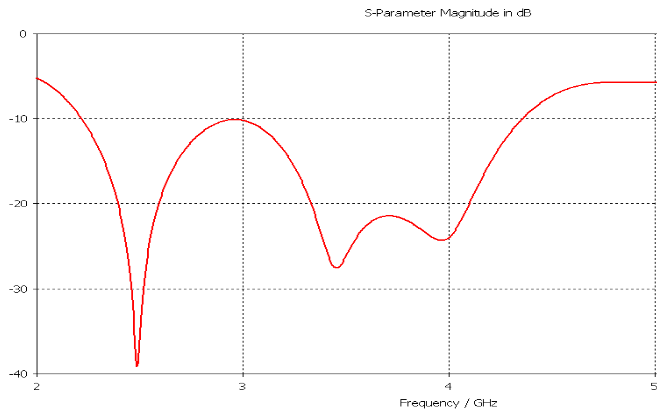

Figure 3. The simulated return loss of the antenna.

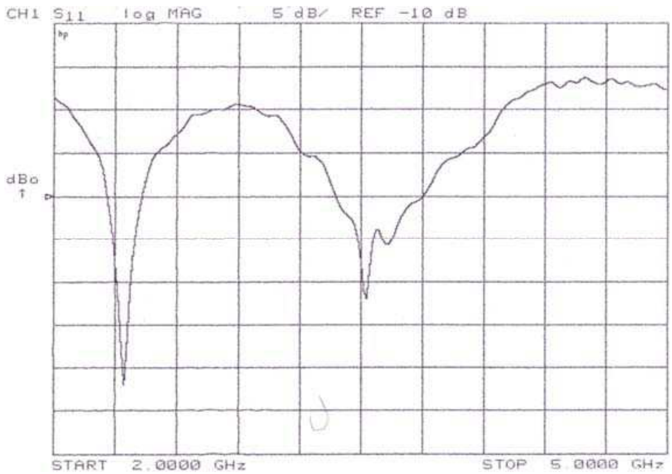

Figure 4. The measured return loss of the antenna.

which make it the most important parameter of all. While "*sd*", "*sdf*", "*w_sd*" control the return loss of the antenna at resonance frequencies. Parameter "*gpd*" is the major influential parameter for deciding the antenna return loss. Varying "*gpd*" results in lowering the return loss on higher frequencies and vice-versa on lower frequencies, so a tradeoff will be assessed in-order to achieve satisfactory performance at both the antenna bands. The parametric variations of all the antennas are shown in Figures 5–9.

Figures 10–11 show the surface current for the above antenna design at 2.4 GHz and 3.5 GHz. The surface current lines at 2.4 GHz

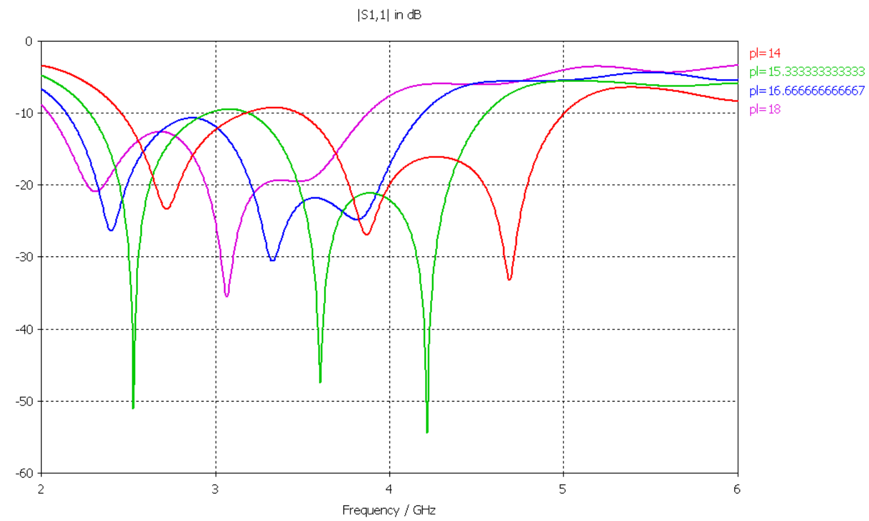

Figure 5. Effect of varying patch length (pl).

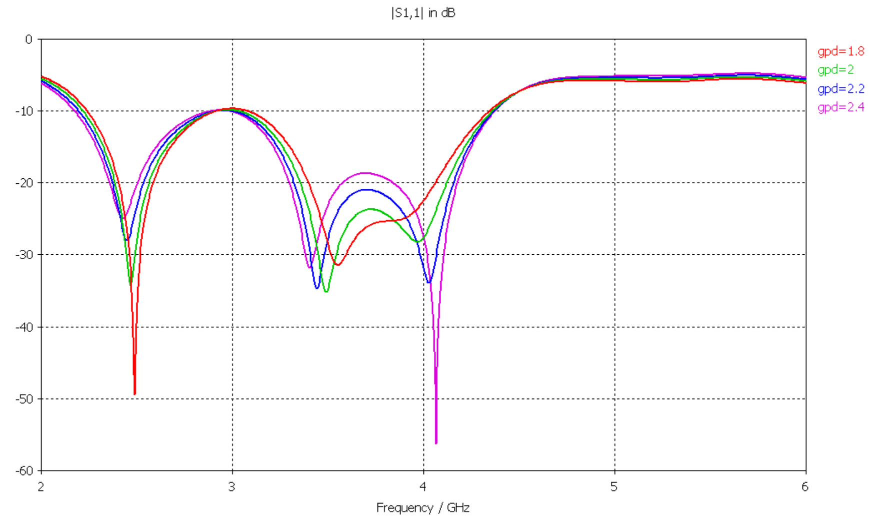

Figure 6. Effect of varying gap between CPW ground plane and patch (gpd).

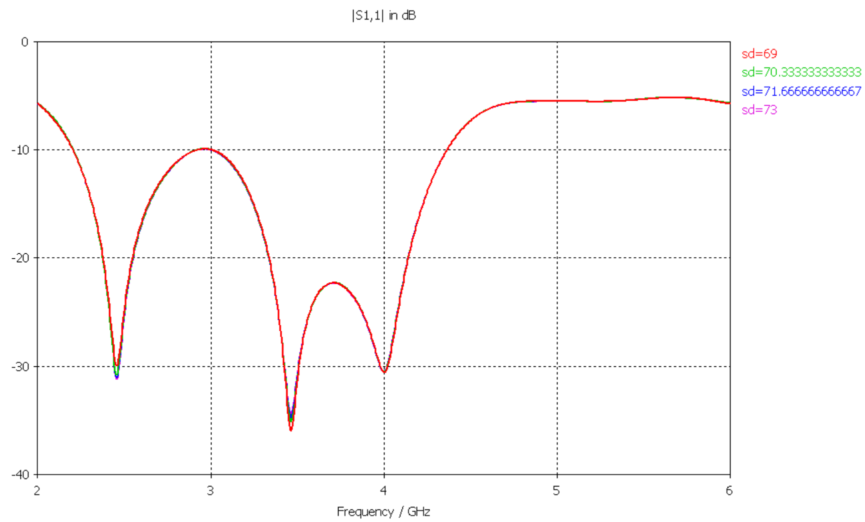

Figure 7. Effect of varying substrate dimension opposite to CPW Feed (sd).

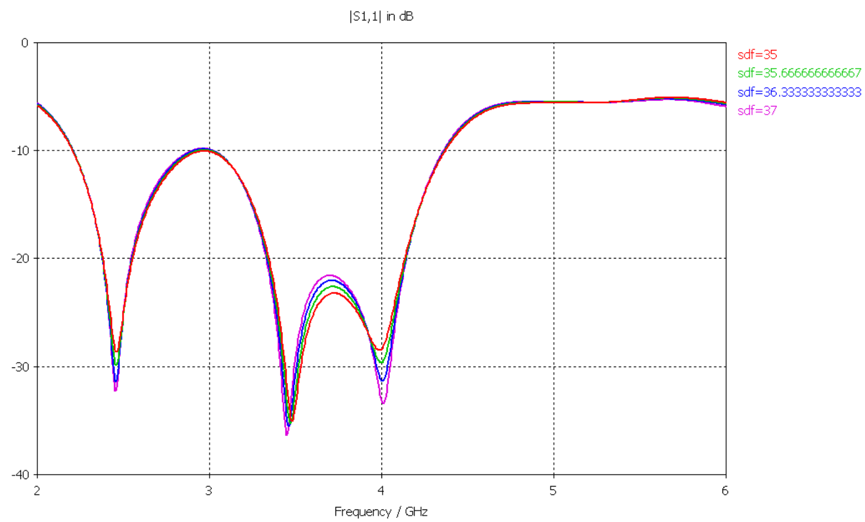

Figure 8. Effect of varying substrate dimension along CPW feed (sdf).

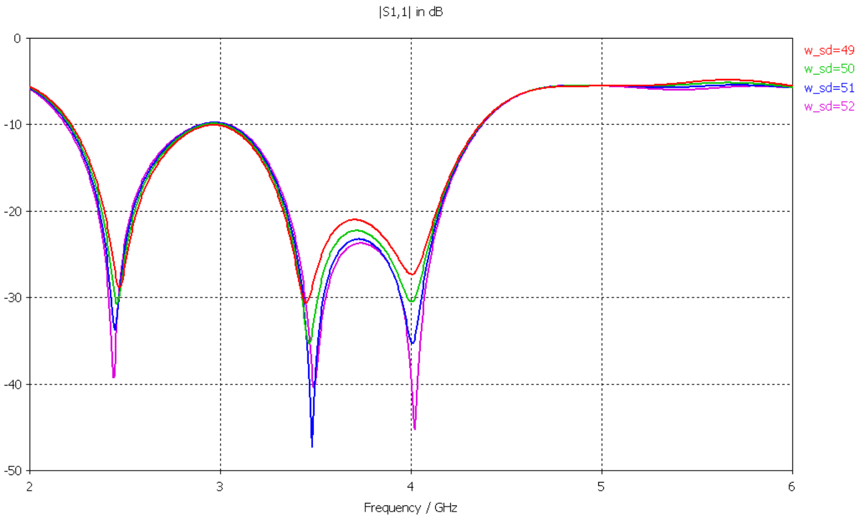

Figure 9. Effect of varying substrate dimension along patch width (w_sd).

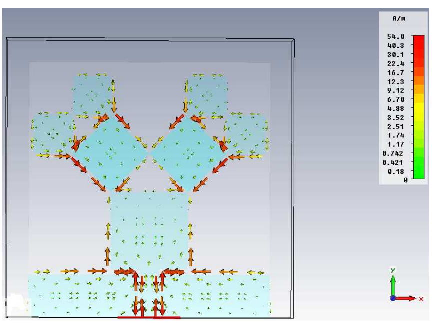

Figure 10. Current distribution at 2.4 Band.

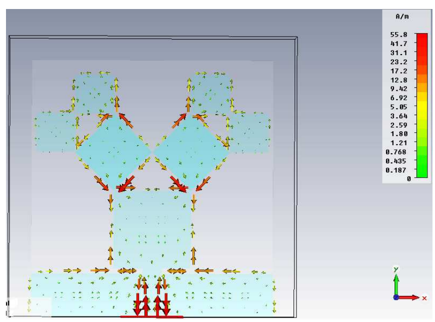

Figure 11. Current distribution at 3.5 GHz.

show that the major contribution for the generation of lower frequency is the patch dimension after the 1st iteration, while surface current lines at frequency 3.5 GHz show that the initiator has the major contribution in the working of antenna at 3.5 GHz. So from current density it is validated that the patch with larger electrical length has smaller frequency, while the patch with smaller electrical length has larger frequency of operation. The antenna is linearly polarized. As the surface currents have almost the same value, there is cross polarization for higher frequency as the surface current lines concentration is more at the edges which are contributing the higher frequency generation.

4. MEASURED RESULTS

The above designed antenna is now fabricated to validate the antenna performance with the simulated antenna. The antenna is fabricated on the Netlec NH9338 ($\varepsilon_r = 3.38$) substrate, and its frequency response was measured on Vector Network Analyzer. Figure 12 shows the fabricated design of the antenna, and Figures 3–4 show the simulated and measured return losses of the antenna. The bandwidth of the fabricated antenna is from 2.15–2.75 GHz for the lower band centered at 2.35 GHz and 3.1–4.2875 GHz for the higher band centered at 3.54 GHz. The results obtained are in agreement with the simulated ones.

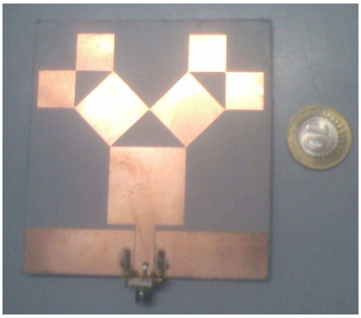

Figure 12. Fabricated antenna using Netlec NH9338 as substrate.

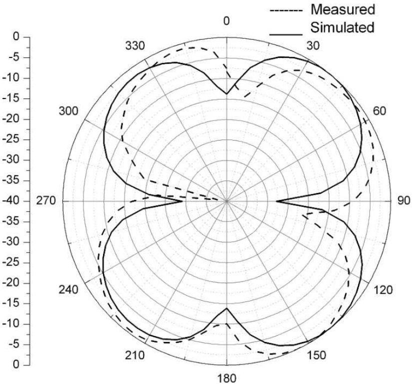

Figure 13. E-plane radiation pattern at 2.4 GHz.

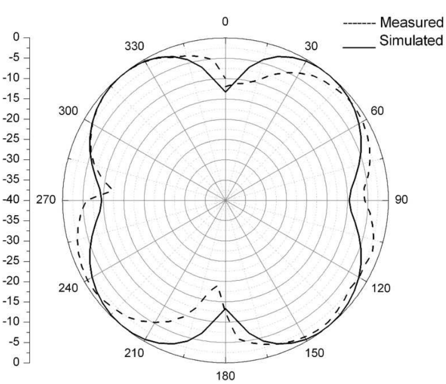

Figure 14. H-plane radiation pattern at 2.4 GHz.

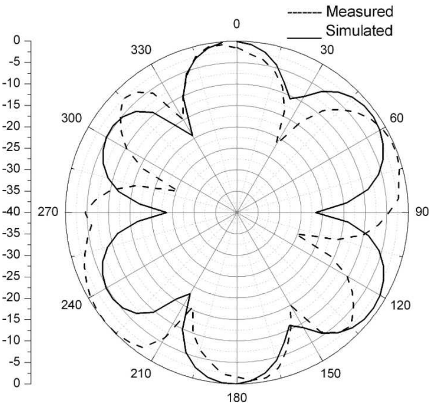

Figure 15. *E*-plane radiation pattern at 3.5 GHz.

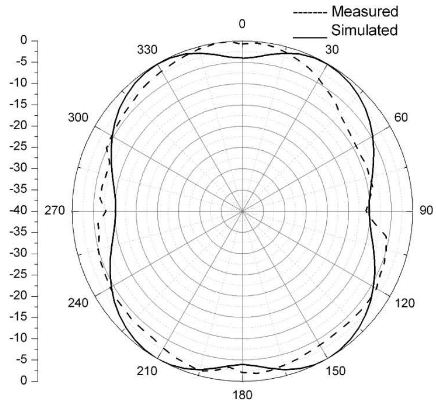

Figure 16. *H*-plane radiation pattern at 3.5 GHz.

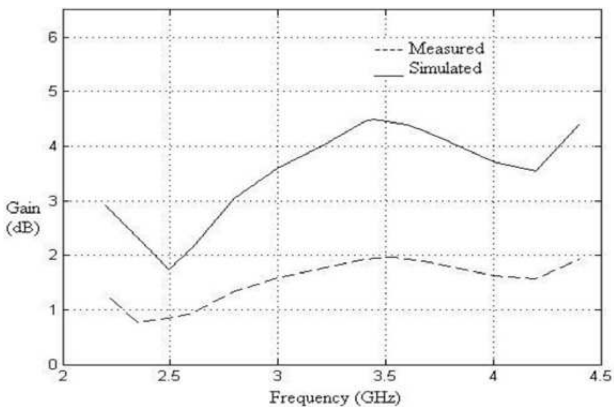

Figure 17. Gains at the 2.4 GHz and 3.5 GHz.

Figures 13–16 show the simulated and measured radiation patterns for E and H-plane at 2.4 GHz and 3.5 GHz. The measured radiation pattern is in good agreement with the simulated one except the H-plane radiation pattern at 3.5 GHz, which is because of measuring the low power levels (levels as low as noise levels) at the antenna in the particular orientation. Gain v/s frequency is one of the ways to assess the antenna performance as shown in Figure 17.

The maximum power levels at both the frequencies are not in broadside direction. At frequency 2.4 GHz the maximum power level is along the 45° with respect to the broadside direction while at 3.5 GHz the maximum power level is along the broadside direction. Consequently, gain measurements are performed for the two frequency bands in the directions of their respective maxima using the substitution/gain-transfer technique with the help of a standard horn antenna with calibrated gain. Figure 17 shows that the measured gain is 1–2 dB less than the simulated gain, which is because of the fabrication and measurement errors.

5. CONCLUSION AND OUTLOOK

A CPW fed Pythagoras tree antenna is simulated, analyzed and fabricated. The antenna shows tremendous potential for wideband applications as it covers WLAN 2.4 GHz band as well as 3.5 GHz WiMAX band. The fabricated design has 25.532% impedance bandwidth in the 1st band and 33.545% impedance bandwidth in the 2nd band with respect to center frequencies of 2.35 GHz and 3.54 GHz respectively. The antenna achieves more than 20% impedance bandwidth at both the frequency bands showing the ultra-wide bandwidth characteristics at both the frequency bands, which was not possible using normal rectangular patch geometry as discussed by authors [12]. The use of fractal geometry (i.e., Pythagoras tree) results in a multi-frequency and ultra-wide bandwidth operation of the antenna without employing any further modification, such as incorporation of U or L slots and stacking techniques which offer an added advantage. However, a supplementary use of such modifications will certainly help in antenna size reduction with a further improved performance.

REFERENCES

1. Basilio, L. I., R. L. Chen, J. T. Williams, and D. R. Jackson, "A new planar dual-band GPS antenna designed for reduced susceptibility to low-angle multipath," *IEEE Transactions on Antennas and Propagation*, Vol. 55, No. 8, 2358–2366, 2007.
2. Lee, C.-J., K. M. K. H. Leong, and T. Itoh, "Compact dual-band antenna using an anisotropic metamaterial," *Proceedings of the 36th European Microwave Conference*, 1044–1047, September 2006.
3. Sze, J.-Y., C.-I G. Hsu, and S.-C. Hsu, "Design of a compact dual-band annular-ring slot antenna," *IEEE Antennas and Wireless Propagation Letters*, Vol. 6, 423–426, 2007.
4. He, S. and J. Xie, "Analysis and design of a novel dual-band array antenna with a low profile for 2400/5800-MHz WLAN systems,"

IEEE Transactions on Antennas and Propagation, Vol. 58, No. 2, 391–396, 2010.

5. Pankhuri and M. V. Kartikeyan, "Full-ψ and half-ψ patch antennas for 2.4/5.8 GHz WLAN application," *Frequenz*, Vol. 64, No. 1–2, 2–9, February 2010.
6. Werner, D. H. and S. Ganguly, "An overview of fractal antenna engineering research," *IEEE Anlennas and Propagation Magazine*, Vol. 45, No. 1, 38–57, 2003.
7. Werner, D. H. and R. Mittra, *Frontiers in Electromagnetics*, IEEE Press, New York, 2000.
8. Gianvittorrio, J. P. and Y. Rahmat-Samii, "Fractal antennas: A novel antenna miniaturization technique and applications," *IEEE Antennas and Propagation Magazine*, Vol. 44, No. 1, 2010.
9. WiMAX Forum, http://www.wimaxforum.org/home/, last visited on June 16, 2010.
10. Ritosa, P., T. Korosec, J. Tratnik, L. Naglic, and B. Batagelj, "Adaptive WiMAX subscriber antenna for 2.6 GHz and 3.45 GHz," *EUROCON 2009*, 46–51, St. Petersburg, Russia, May 2009.
11. Prombutr, N. and P. Akkaraaektharin, "Analysis and design hilbert curve fractal antenna feed with co-planar waveguide for multi-band wireless communication," *International Journal of Engineering*, Vol. 2, No. 3, 1–11, May/June 2008.
12. Dafalla, Z. I., W. T. Y. Kuan, A. M. Abdel Rahman, and S. C. Shudakar, "Design of a rectangular microstrip patch antenna at 1 GHz," *RF and Microwave Conference*, 145–149, 2004.
13. Tiwari, H. and M. V. Kartikeyan, "A stacked microstrip patch antenna with fractal shaped defects," *Progress In Electromagnetic Research C*, Vol. 14, 185–195, July 2010.
14. Aggarwal, A. and M. V. Kartikeyan, "Design of sierpinski carpet antenna using two different feeding mechanisms for WLAN applications," *Int. Conf. Infrared, Millimeter, and THz Waves 2010*, Rome, Italy, September 5–10, 2010 (accepted).